

Supersymmetric Analysis of Stochastic Micro-Bending in Optical Waveguides*

Stuart Ward^{1,2}, Rouzbeh Allahverdi¹, and Arash Mafi^{1,2†}

¹*Department of Physics & Astronomy, University of New Mexico, Albuquerque, NM 87106, USA.*

²*Center for High Technology Materials, University of New Mexico, Albuquerque, New Mexico 87106, USA.*

(Dated: August 9, 2021)

Micro-bending attenuation in an optical waveguide can be modeled by a Fokker-Planck equation. It is shown that a supersymmetric transformation applied to the Fokker-Planck equation is equivalent to a change in the refractive index profile, resulting in a larger or smaller attenuation. For a broad class of monomial index profiles, it is always possible to obtain an index profile with a larger micro-bending attenuation using a supersymmetric transformation. However, obtaining a smaller attenuation is not always possible and is restricted to a subset of index profiles.

I. INTRODUCTION

Supersymmetric Quantum Mechanics (SUSY-QM) was first introduced as a toy model to study SUSY breaking [1], and has since evolved into a powerful theoretical framework with many applications in theoretical physics [2–7]. Such applications include the classification of potentials with identical spectra [8], analytical derivation of spectra in certain classes of quantum Hamiltonians [9], extensions to the WKB approximation [10], analysis of the Fokker-Planck equation (FPE) in statistical mechanics [7], and random matrix theory [11], disorder, and chaos [12]. Using the close analogy between the Schrödinger equation for a particle in a potential and light propagation in a dielectric medium, SUSY-QM has also been employed extensively in various optical waveguide designs and optical scattering problems over the past few years [13–25].

Another application of SUSY-QM is in the analysis of classical stochastic dynamics with one Cartesian degree of freedom [7, 26, 27]. It uses the fact that the FPE can be mapped into an imaginary-time Schrödinger equation

$$-\frac{\partial}{\partial t}\Psi_{\pm}(t, x) = H_{\pm}\Psi_{\pm}(t, x), \quad (1)$$

where $H_{\pm} = -\partial_x^2 + W^2(x) \pm W'(x)$ are the partner Hamiltonians in the Witten's model, and $W(x)$ is the superpotential. The eigenvalues of H_{\pm} are the decay rates associated with the eigenfunctions of the imaginary-time Schrödinger equation. In the presence of an unbroken SUSY, H_+ and H_- have identical positive eigenvalues (positive decay rates), while H_- has an additional vanishing eigenvalue, corresponding to its ground-state. In this paper, we explore how this formalism can be used to solve practical problems in classical stochastic optics. In particular, we consider the problem of micro-bending in optical waveguides, which is an important issue affecting the optical communications networks [28, 29]. Undesirable

fiber-fiber and fiber-cable interactions, caused by manufacturing of fiber cables or thermal-induced variations, result in random microscopic bends leading to signal loss. The estimation of microbending loss has been performed in various publications. In particular, Jin and Payne [29] have presented a detailed numerical investigation, based on an analytical model, and have validated the model by comparing with experimental measurements. Therefore, there is a good coverage on the estimation of microbending loss in the existing literature. Our intention here is not to present a new way of estimating microbending attenuation; rather, this paper is framed around using SUSY-QM to design an optical waveguide with a reduced micro-bending loss. Moreover, the overall formalism and ideas can be readily applied to a wide range of problems involving stochastic dynamics.

II. OPTICAL WAVEGUIDE WITH MICRO-BENDING

An optical waveguide is a transversely inhomogeneous structure, usually containing a region of increased refractive index, compared with the surrounding medium. Here, to illustrate the main ideas, we consider the micro-bending of a planar waveguide structure. Generalization to an optical fiber is possible but is beyond the scope of the present work. We note that intrinsic fluctuations in the refractive index, including those stemming from random glass density fluctuations or the presence of impurities, lead to unwanted back-scattering and mode mixing. For the case of micro-bending, the refractive index fluctuation is not intrinsic but can be modeled as a modification of the refractive index by the addition of a linear term to the first order in the radial coordinate over the radius of the curvature. Such a tilt in the refractive index profile results in leaking radiation.

For the problem of interest, we assume a planar waveguide structure defined by an inhomogeneous refractive index $n(y)$, which is independent of the x and z coordinates. The light rays are confined in the y direction by the inhomogeneous refractive index, while propagating freely in the z direction. The trajectories of light rays are determined by Fermat's principle [30], $\delta \int_a^b n(y) ds = 0$,

* This research is supported by grant number W911NF-19-1-0352 from the United States Army Research Office.

† mafi@unm.edu

where ds is the differential length on a trajectory between points a and b in the $y-z$ plane. Using the calculus of variation results in the following differential equation for the ray trajectory $y(z)$:

$$\frac{d}{ds} \left(n \frac{dy}{ds} \right) = \frac{\partial n}{\partial y}, \quad ds = \sqrt{dy^2 + dz^2}. \quad (2)$$

To model the micro-bending, we assume that the optical waveguide is bent in the $y-z$ plane with a local curvature of $\kappa(z)$. A bent waveguide can be conformally mapped to a straight waveguide, where the effect of the local bending can be modeled as a variation in the refractive index [31, 32] given by $n(y, z) \approx n_s(y) [1 - \kappa(z)y]$. n_s is the effective refractive index for the straight waveguide (without micro-bending). In the paraxial approximation, the ray trajectory is almost parallel to the z axis, so we can assume $ds \approx dz$. Moreover, the maximum of the refractive index is commonly at or near the waveguide center at $y = 0$, and the refractive index gradually decreases away from the center. Taking these points into consideration and in the absence of large transverse variations, the ray propagation equation can be simplified into the dynamical equation of a point particle subject to a net force of $F(y) - \kappa(z)$, where the conservative force $F(y)$ is exclusively due to the inhomogeneous refractive index $n_s(y)$ [33, 34]:

$$\frac{d^2 y}{dz^2} \approx F(y) - \kappa(z). \quad (3)$$

Note that the longitudinal coordinate z plays the role of time for the point particle. The conservative force $F(y)$ is related to the effective potential $U(y)$ by

$$F(y) = -dU/dy, \quad U(y) = 1 - n_s(y)/n_0, \quad (4)$$

where $n_0 = n_s(y = 0)$ and $U(0) = 0$. Because the refractive index decreases away from the center of the waveguide, the potential increases at large $|y|$ and $U(y)$ is a confining potential.

We assume that the waveguide curvature $\kappa(z)$ is a zero mean ($\langle \kappa(z) \rangle = 0$) white stochastic process with the autocorrelation given by

$$\langle \kappa(z)\kappa(z') \rangle = \kappa_0^2 \delta(z - z'). \quad (5)$$

The ray propagation equation (3) can be expressed as a stochastic Langevin equation in the following form:

$$\frac{dy}{dz} = \theta(z), \quad \frac{d\theta}{dz} = F(y) - \kappa(z), \quad (6)$$

where $\theta(z)$ is the local angle of the ray relative to the z axis. Instead of solving Eq. (6) for each random realization and then averaging the results, it is more convenient to use the corresponding FPE, from which we can determine the probability P of an optical ray to be at lateral position y and angle θ at point z along the fiber [33, 34]:

$$\left[\frac{\partial}{\partial z} + \theta \frac{\partial}{\partial y} + F \frac{\partial}{\partial \theta} - \frac{\kappa_0^2}{2} \frac{\partial^2}{\partial \theta^2} \right] P(y, \theta, z) = 0. \quad (7)$$

The FPE (7) describes many stochastic problems in the phase-space; therefore, the following results can be applied to a wide range of physical systems beyond the micro-bending problem that is analyzed here.

This can be further simplified by noting that the Hamiltonian of the conservative system (in the absence of stochastic noise) is given by

$$E = \frac{1}{2}\theta^2 + U(y), \quad (8)$$

where θ plays the role of the velocity of the point particle with the mass $m = 1$. In a typical graded-index optical waveguide, where the refractive index peaks in the center of the waveguide and gradually decreases away from the center, light rays follow sinusoidal-like paths along the waveguide. In the center where U is zero, the angle θ and the kinetic term assume their maximum values. As a ray reaches its maximum transverse separation from the center and bends back towards the center, θ and the kinetic term become zero and U reaches its maximum value equal to E . In other words, E determines the maximum ray angle at the center and also the maximum distance a ray can reach away from the center. Of course, if the energy E of a light ray is too large, it can breach the potential barrier into free space. In the modal language of wave optics, the energy E can be related to the mode number, where a larger E corresponds to a higher order mode and the energy at which a light ray breaches the potential barrier corresponds to the highest order mode supported by the waveguide. In Eq. (7), the microbending attenuation appears as the exponential decay of the probability $P(y, \theta, z)$ with respect to the propagation distance z as will be discussed in detail later in the paper.

The phase-space action, which is a conserved quantity, is the area enclosed in the phase-space by the ray trajectory and is given as

$$I(E) = \oint_T d\theta dy = \oint_T \sqrt{2[E - U(y)]} dy = T\bar{\theta}^2, \quad (9)$$

where T is the ray period and overbar denotes the average over one ray period. The derivative of I with respect to E also takes the simple form of

$$I'(E) = \oint_T \frac{1}{\sqrt{2(E - U)}} dy = T. \quad (10)$$

Using this information, the FPE in (7) can be expressed in a much simpler form, where y and θ are swapped with a single variable E to obtain

$$\frac{2}{\kappa_0^2} \frac{\partial P(E, z)}{\partial z} = -\frac{\partial P(E, z)}{\partial E} + \frac{\partial^2 [\mathbb{Z}(E)P(E, z)]}{\partial E^2}, \quad (11)$$

where $P(E, z)$ is the probability of the ray to have energy E at point z along the waveguide, and $\mathbb{Z}(E) = I(E)/I'(E)$ is twice the average kinetic energy over one ray period.

We now make a change of variable (both in E and P) and transform the FPE in (11) to an imaginary-time Schrödinger equation, similar to Eq. (1). We write $E = E(\mathcal{E})$ and $P(E, z) = B(E)Q(E, z)$ and choose the function $E(\mathcal{E})$ and the form of $B(E)$ to satisfy

$$\mathbb{Z}\mathcal{E}'^2 = 1, \quad \mathbb{Z} = \dot{E}^2, \quad 2\mathbb{Z}B' + \left(\frac{3}{2}\mathbb{Z}' - 1\right)B = 0, \quad (12)$$

where \prime and $\dot{}$ denote differentiation with respect to E and \mathcal{E} , respectively. The solutions to these equations are formally given by

$$\begin{aligned} \mathcal{E} &= \int \frac{dE}{\sqrt{\mathbb{Z}}}, & E &= \int \sqrt{\mathbb{Z}} d\mathcal{E}, & (13) \\ B &= \mathbb{Z}^{-3/4} \exp\left(\int \frac{dE}{2\mathbb{Z}}\right). \end{aligned}$$

Using these changes of variables, we arrive at the imaginary-time Schrödinger equation

$$-\frac{\partial Q}{\partial \mathbb{Z}} = -\frac{\partial^2 Q}{\partial \mathcal{E}^2} + V(\mathcal{E})Q, \quad (14)$$

where $Z = \kappa_0^2 z/2$ and

$$V(\mathcal{E}) = \mathbb{F}^{-1} \frac{\partial^2}{\partial \mathcal{E}^2} \mathbb{F}, \quad \mathbb{F}^4 = [I^2(E)]' = 2[\dot{I}(\mathcal{E})]^2. \quad (15)$$

We now have all the required ingredients to make a SUSY transformation on Eq. (14). Once we find the SUSY partner potential to $V(\mathcal{E})$, we can work our way backward to find the corresponding $I(E)$ from Eq. (15) and consequently $Z(E)$, from which we can find $U(y)$. This will be achieved by using the Abel transform-pairs, which can be expressed as

$$I'(E) = \int_0^E \left(\frac{2\sqrt{2}}{\partial_y U}\right) \frac{dU}{\sqrt{E-U}}, \quad (16)$$

$$\frac{2\sqrt{2}}{\partial_y U} = \frac{1}{\pi} \frac{\partial}{\partial U} \int_0^U I'(E) \frac{dE}{\sqrt{U-E}}. \quad (17)$$

Note that Eq. (16) is essentially the same as Eq. (10), albeit with a change of variable. Equation (17) gives us the required information about the new $U(y)$. In other words, the Abel transform-pairs allow us to relate the phase-space action to the refractive index profile of the optical waveguide and vice versa.

Example of a monomial potential: As a concrete example we explore a monomial potential of the form $U(y) = \Delta|y/y_c|^\alpha$ in some detail. This model arises in graded-index optical waveguides [35, 36], where y_c is the waveguide half-width, α controls the shape of the index profile, and Δ determines the refractive index contrast of the center relative to the core edges at $y = \pm y_c$. Note that it is common to take $\alpha \approx 2$ in practical optical waveguides [35, 36], because it reduces the modal dispersion in optical waveguides by equalizing the group velocities of

the modes. In the ray picture, for $\alpha \approx 2$, all rays of different energy E (and maximum value of θ) reach the end of the waveguide at the same time.

In the following discussion, because the potential is assumed to be symmetric under $y \rightarrow -y$, we only consider the $y \geq 0$ region without loss of generality. For this problem, we can evaluate $I(E)$ using

$$\begin{aligned} I(E) &= \int_0^E \left(\frac{4\sqrt{2}}{\partial_y U}\right) \sqrt{E-U} dU & (18) \\ &= \frac{\sqrt{8\pi} \Gamma(1+1/\alpha)}{\Gamma(3/2+1/\alpha)} y_c \Delta^{-1/\alpha} E^{1/\zeta}, \quad \text{where } \zeta = \frac{2\alpha}{\alpha+2}. \end{aligned}$$

In this special case, the ratio $\mathbb{Z}(E)$ takes the simple form of $\mathbb{Z}(E) = \zeta E$, and we obtain $4E = \zeta \mathcal{E}^2$ and $B^{2\alpha} \propto E^{(1-\alpha)}$. Using these results and Eq. (15), we obtain:

$$V(\mathcal{E}) = \frac{1-\alpha}{\alpha^2 \mathcal{E}^2} = \frac{\nu^2 - 1/4}{\mathcal{E}^2}, \quad \text{where } \nu = \frac{2-\alpha}{2\alpha}. \quad (19)$$

Before we present the solution to Eq. (14), we note that lossy rays are those which can breach the potential barrier into the free space, i.e. with an energy larger than a given \mathbb{E} . This results in a boundary condition of $P(\mathbb{E}, z) = 0$, or equivalently $Q(\epsilon, Z) = 0$, where $4\mathbb{E} = \zeta \epsilon^2$. Attempting an eigensolution of the form $Q(\mathcal{E}) = Q_m(\mathcal{E})e^{-\lambda_m Z}$, we obtain

$$Q_m(\mathcal{E}) = \sqrt{\mathcal{E}/\epsilon} J_\nu(\sqrt{\lambda_m} \mathcal{E}), \quad \lambda_m = u_{\nu m}^2/\epsilon^2, \quad (20)$$

where J_ν is the Bessel function of order ν and $u_{\nu m}$ is the m th zero of J_ν , where $m = 0, 1, \dots$. Recall that $Z = \kappa_0^2 z/2$, where κ_0 is defined through the autocorrelation of the curvature which is defined in Eq. (5). The relationship between attenuation and curvature can now be seen from the term $e^{-\lambda_m Z}$ of the above eigensolution. Furthermore, recall that the goal of performing the SUSY transformation is to find a new potential which possesses an additional eigensolution with a decay constant that is smaller than the smallest decay constant (λ_0) of the above eigensolution.

To perform a SUSY transformation, we need to calculate the superpotential $W = -\dot{Q}_0/Q_0$, where Q_0 is the eigensolution with the smallest decay coefficient, i.e. λ_0 . We obtain

$$W = -\frac{\nu+1/2}{\mathcal{E}} + \sqrt{\lambda_0} \frac{J_{\nu+1}(\sqrt{\lambda_0} \mathcal{E})}{J_\nu(\sqrt{\lambda_0} \mathcal{E})}. \quad (21)$$

The partner potentials are derived from $V_\pm = W^2 \pm \dot{W}$. We obtain

$$V_- = -\lambda_0 + \frac{\nu^2 - 1/4}{\mathcal{E}^2}, \quad (22)$$

$$V_+ = +\lambda_0 + \frac{\mathcal{G}}{\mathcal{E}^2}, \quad (23)$$

$$\mathcal{G} = \frac{3}{4} + \nu(\nu+2) - \frac{(4\nu+2)\sqrt{\lambda_0} \mathcal{E} J_{\nu+1}}{J_\nu} + \frac{2\lambda_0 \mathcal{E}^2 J_{\nu+1}^2}{J_\nu^2},$$

where we have suppressed the argument of the Bessel functions, all being $\sqrt{\lambda_0}\mathcal{E}$. Note that V_- is the same as the potential in Eq. (19) except it is shifted by λ_0 as expected [37]. We also have $\lambda_0 = u_{\nu 0}^2/\epsilon^2$; therefore, we are only interested in V_{\pm} in the range of $0 \leq \mathcal{E} < \epsilon$, where V_+ blows up at the upper boundary.

To establish a concrete numerical example, we consider the case of a quadratic graded index with $\alpha = 2$ and $\nu = 0$, where $u_{00} \approx 2.405$. We assume that those rays that can make it to $y \geq y_c$ are lost to free space, resulting in $\mathbb{E} = \Delta$ or equivalently $\epsilon = 2\sqrt{\Delta}$. We also assume $\Delta = 0.01$, which is a reasonable value in graded index optics, resulting in $\epsilon = 0.2$ and $\lambda_0 \approx 144.58$. In this case, we plot V_{\pm} from Eqs. (22) and (23), except we redefine these functions by adding λ_0 to get the original V_- back. These shifted potentials are plotted in FIG. 1. In physical units, the lowest attenuation coef-

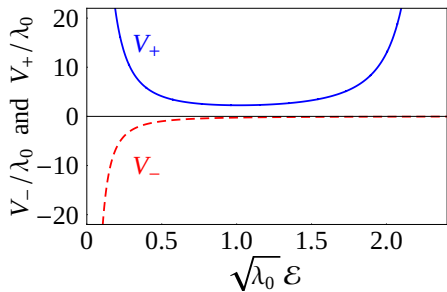


FIG. 1. V_{\pm} from Eqs. (22) and (23) are plotted as a function of $\sqrt{\lambda_0}\mathcal{E}$ for $\nu = 0$. The potentials are shifted up by λ_0 and are expressed in units of λ_0 .

ficient corresponds to $\lambda_0\kappa_0^2/2$. Considering a waveguide with $y_c \approx 1\mu\text{m}$ and $\kappa_0^2 \approx 4.8 \times 10^{-6}\mu\text{m}^{-1}$, which corresponds to a fluctuation in radius of curvature of $457\mu\text{m}$ over a longitudinal distance comparable to y_c , the lowest attenuation is obtained to be around 3dB/mm. Less fluctuation corresponds to larger curvature radii fluctuating at a slower rate with the propagation distance.

To verify that V_+ is a true superpartner potential to V_- , we solve the eigenvalue problem with V_+ in Eq. (14) assuming the Z -dependence of the form $e^{-\lambda_m Z}$ and the Dirichlet boundary condition: $Q^+(0) = Q^+(\epsilon) = 0$ (superscript $+$ signifies its correspondence to V_+). The eigenvalues must match those of the excited states obtained from V_- . We plot, in FIG. 2(a), the lowest 4 eigenfunctions Q_m^- ($m = 0, 1, 2, 3$) corresponding to V_- from Eq. (20), where m corresponds to how many times the eigenfunction crosses the $Q = 0$ horizontal axis. The corresponding eigenvalues are $\lambda_m = (u_{0m}/u_{00})^2\lambda_0$ for $m = 0, 1, 2, 3$, respectively. Similarly, in FIG. 2(b), we plot the lowest 3 eigenfunctions Q_m^+ ($m = 1, 2, 3$) corresponding to V_+ that are evaluated numerically, where $m - 1$ corresponds to the number of crossings with the $Q = 0$ horizontal axis. It can be confirmed, numerically, that the eigenvalues corresponding to Q_1^+ , Q_2^+ , and Q_3^+

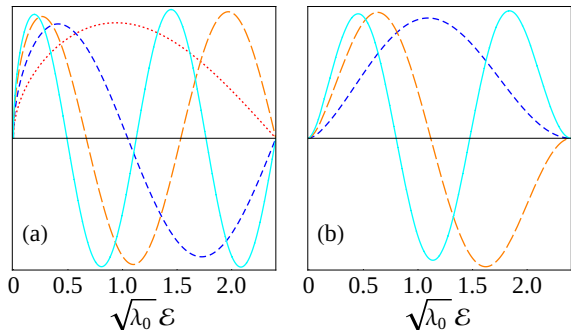


FIG. 2. (a) The lowest 4 eigenfunctions Q_m^- ($m = 0, 1, 2, 3$) corresponding to V_- , and (b) the lowest 3 eigenfunctions Q_m^+ ($m = 1, 2, 3$) corresponding to V_+ are plotted.

match those of Q_1^- , Q_2^- , and Q_3^- , respectively, as expected from an unbroken SUSY.

We now outline the procedure to evaluate $U(y)$ corresponding to V_+ . We first insert V_+ from Eq. (23) into Eq. (15) and obtain a numerical solution for \mathbb{F} . The boundary conditions for \mathbb{F} are set at $\mathcal{E} \rightarrow 0$: we make a Taylor expansion of V_+ near this point and analytically solve Eq. (15) near $\mathcal{E} = 0$ to find that $\mathbb{F}(\mathcal{E}) \propto \mathcal{E}^{3/2}$ and $\dot{\mathbb{F}}(\mathcal{E}) \propto (3/2)\mathcal{E}^{1/2}$. These expressions guide us to set the boundary conditions for \mathbb{F} and $\dot{\mathbb{F}}$ for $\mathcal{E} \rightarrow 0$. Note that Eq. (15) can determine \mathbb{F} only up to an overall factor, and this is rooted in the fact that $I(E)$ in Eq. (9) can be multiplied by a constant factor without changing the FPE. The next step is to use $\sqrt{2}\dot{I} = \mathbb{F}^2$, assuming that $I(0) = 0$, to numerically evaluate $I(\mathcal{E})$. It can be shown that $\mathbb{Z}(\mathcal{E}) = 2I^2/\mathbb{F}^4$, so we use this expression to evaluate $\mathbb{Z}(\mathcal{E})$. Next, $\mathbb{Z}(\mathcal{E})$ along with the transformations in Eq. (13) are used to relate E to \mathcal{E} . Using this relationship and $I(\mathcal{E})$, we can find $I(E)$ and consequently $I'(E)$, to be used in Eq. (17) to find $U(y)$. Considering that $U(y = 0) = 0$, we can rewrite Eq. (17) in the simpler form of

$$y = \frac{1}{2\sqrt{2}\pi} \int_0^U I'(E) \frac{dE}{\sqrt{U-E}}. \quad (24)$$

Because the redundant multiplicative factor mentioned earlier propagates to $I'(E)$ in Eq. (24), the right-hand side of Eq. (24) can only be determined up to an overall factor. This ambiguity is there because nowhere in our formalism did we use the actual value of y_c , so we can normalize the result obtained in Eq. (24) to y_c . The final result is shown in Fig. 3, where U_- corresponds to V_- and is given by $\Delta(y/y_c)^2$, and U_+ corresponds to V_+ and is obtained according to the numerical procedure outlined above. We remind that because these potentials are symmetric under $y \rightarrow -y$, only the $y \geq 0$ region is shown in Fig. 3. Note that U_- is quadratic and concave; however, U_+ is convex and its derivative at $y = 0$ blows up. In practical situations, a slightly rounded potential

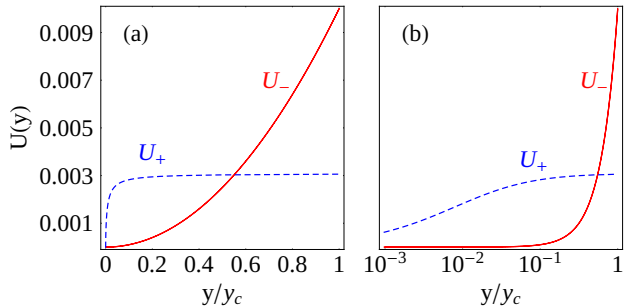


FIG. 3. (a) $U_- = \Delta(y/y_c)^2$ (corresponding to V_-) is plotted in comparison to U_+ (corresponding to V_+), where U_+ is obtained according to the outlined numerical procedure. Plots in (b) are the same as (a) but the vertical axis is logarithmic. Note that $V_{-,-}$ and $U_{-,-}$ do not exist for the case of $\alpha = 2$ treated here.

at $y = 0$ does not alter the behavior of the system in a notable way.

Let us recap the behavior of the two systems as $\mathcal{E} \rightarrow 0$. For V_- , $\mathbb{F} \propto \mathcal{E}^{1/2}$, so $\dot{I} \propto \mathcal{E}$ and $I \propto \mathcal{E}^2$. Therefore, $\mathbb{Z} \propto \mathcal{E}^2$, which results in $E \propto \mathcal{E}^2$. As such, $I \propto E$ and $I' = \text{const.}$, which results in $\partial_y U = 0$ for $y \rightarrow 0$ according to Eq. (17). On the other hand, for V_+ , $\mathbb{F} \propto \mathcal{E}^{3/2}$, so $\dot{I} \propto \mathcal{E}^3$ and $I \propto \mathcal{E}^4$. Therefore, $\mathbb{Z} \propto \mathcal{E}^2$, which results in $E \propto \mathcal{E}^2$. As such, $I \propto E^2$ and $I' \propto E$, which results in $|\partial_y U| \rightarrow \infty$ for $|y| \rightarrow 0$ according to Eq. (17). The lowest order decay coefficient for U_+ is $\lambda_1 = (u_{01}/u_{00})^2 \lambda_0$, which is larger than that of U_- (λ_0) and this agrees with the form of U_+ and the fact that it is shallower than U_- .

III. LOWERING THE LOSS

We would now like to carry out the reverse operation and find out if there exists a SUSY-constructed potential, which we refer to as $U_{-,-}$, that can result in a lower minimum attenuation than λ_0 . To achieve this, one must find a potential $V_{-,-}$ that is the superpartner potential to (a slightly shifted) V_- but with a lower (zero energy) ground state. This implies that we need to find a W that satisfies $W^2 + \dot{W} = V_-$, where the positive sign behind \dot{W} implies that V_- is the higher energy superpartner potential, and $W^2 - \dot{W} = V_{-,-}$.

It is seen from Eq. (19) that regardless of a finite shift in V_- , the behavior of V_- for $\mathcal{E} \rightarrow 0$ is of the form $(\nu^2 - 1/4)/\mathcal{E}^2$. Previously, setting $W^2 - \dot{W} = V_-$ resulted in $W \sim -(\nu + 1/2)/\mathcal{E}$, consistent with Eq. (21) for $\mathcal{E} \rightarrow 0$ and $Q_0 \sim \mathcal{E}^{1/2+\nu}$ with a Dirichlet boundary condition for Q_0 at $\mathcal{E} = 0$. For $\alpha > 0$, $\nu > -1/2$, and hence Q_0 is always well-behaved for $\mathcal{E} \rightarrow 0$, which is reassuring. Now, setting $W^2 + \dot{W} = V_-$ results in $W \sim (1/2 - \nu)/\mathcal{E}$. As such, the ground state of $V_{-,-}$, which would have to

satisfy $W = -\dot{Q}_0/Q_0$ gives $Q_0 \sim \mathcal{E}^{-1/2+\nu}$. This form of Q_0 is only non-diverging for $\mathcal{E} \rightarrow 0$, and hence normalizable, if $\nu > 1/2$. This happens if $\alpha < 1$, which implies $V_{-,-}$ can be found only if $\nu > 1/2$ (equivalently $\alpha < 1$).

This clearly shows that for the quadratic potential $\Delta(y/y_c)^2$, with $\nu = 0$ and $\alpha = 2$, there exists no $V_{-,-}$. In other words, one cannot find a lower energy superpartner potential that results in a lower micro-bending attenuation. However, for $\Delta(y/y_c)^\alpha$ with $\alpha < 1$ which is of the concave form, $V_{-,-}$ can be found. It can be used to construct a potential $U_{-,-}$, and hence a refractive index that has a lower micro-bending attenuation. The evidence of this already exists in our calculations. Previously, we used $\nu = 0$ for V_- in Eq. (22), corresponding to $U_- = \Delta(y/y_c)^2$, to construct V_+ in Eq. (23) corresponding to U_+ . As such, one expects to be able to construct V_- from V_+ . To reverse the logic, we note that the behavior of V_+ for $\mathcal{E} \rightarrow 0$ is of the form $V_+ \sim (3/4)/\mathcal{E}^2$ for $\mathcal{E} \rightarrow 0$. Because $\nu^2 - 1/4 = 3/4$ results in $\nu = 1 > 1/2$, so it is no wonder that V_- exists as the lower energy partner of V_+ .

Using these results, we can make general arguments on how the shape of U changes under SUSY transformations, both going up (V_- to V_+) and possibly going down (V_- to $V_{-,-}$). Recall that $W^2 - \dot{W} = (\nu^2 - 1/4)/\mathcal{E}^2$ results in $W \sim -(\nu + 1/2)/\mathcal{E}$, while $W^2 + \dot{W} = (\nu'^2 - 1/4)/\mathcal{E}^2$ results in $W \sim (1/2 - \nu')/\mathcal{E}$. Thus, for an “up-ward” SUSY transformation $\nu' = \nu + 1$ or, equivalently, $\alpha' = \alpha/(1 + \alpha)$. We have already seen this for $\nu = 0$ and $\alpha = 2$ in V_- , which resulted in $\nu' = 1$ and $\alpha' = 2/3$ in V_+ . In fact, it can be shown that U_+ scales as $\sim (y/y_c)^{2/3}$ near $y = 0$. The relation $\alpha' = \alpha/(1 + \alpha)$ shows that in an “up-ward” SUSY transformation the power in the potential of the form $U \sim (y/y_c)^\alpha$ decreases and the potential becomes (more) concave. Another important point is that the “up-ward” SUSY transformation is always permitted [37]. On the other hand, for a “down-ward” SUSY transformation, i.e. for V_- going down to $V_{-,-}$, we have $\alpha' = \alpha/(1 - \alpha)$. First, $\alpha < 1$ is required for this to make sense, as we showed above, and the potential becomes (more) convex under this operation. For example, $\alpha = 1/2$ in V_- gives $\alpha' = 1$ for $V_{-,-}$.

We would like to emphasize two important points regarding the results obtained in this paper. First, we make a general observation that the attenuation can be lowered only in profiles with $\alpha < 1$. In particular, for the interesting case of $\alpha \approx 2$, lowering the attenuation is not possible. However, our results are strictly true only for monomial index profiles and we have not explored other forms. Therefore, we are not ruling out the possibility that a SUSY transformation can be used to lower the attenuation for a non-monomial near-quadratic index profile. Second, our conclusions are based only on SUSY transformations and we are not ruling out the possibility of lowering the attenuation for the monomial index profile with $\alpha > 1$ by leveraging other non-SUSY transformations. In practical optical waveguide designs (especially for optical fibers), some common values of α are $\alpha \gg 1$ for a step-

index waveguide, $\alpha \approx 2$ for a graded-index waveguide to reduce the modal dispersion, and $\alpha \approx 1$ for a dispersion-shifted waveguide [38]. One can envision $\alpha < 1$ profiles for dispersion shifting as well. However, considering that $\alpha < 1$ is not a commonly used profile, our finding can be considered as a “negative result”, showing that the attenuation of commonly used optical waveguides cannot be reduced by a SUSY transformation, subject to the limitations stated above.

IV. CONCLUSIONS

We have employed SUSY-QM in the analysis of a classical stochastic optics problem: the random microbending loss of a waveguide. For a general class of monomial-shaped potentials (refractive index profile), we showed that a SUSY transformation can always be used to make the waveguide more lossy (V_- to V_+), but only certain refractive index profiles are amenable to a (re-

verse) SUSY transformation to make the waveguide less lossy (V_- to $V_{-, -}$). The results of this paper can potentially be used as a seed for the optimization or inverse design of optical waveguides. Our work may also serve as a framework to investigate similar phenomena in optics or other areas of physics described by a FPE that can be investigated by using the SUSY-QM formalism.

We would like to emphasize that our work is performed using the geometrical ray picture in what effectively constitutes a highly multimode waveguide. We would like to acknowledge the interesting result obtained in Ref. [39] on the loss due to sidewall roughness for single mode propagation. Their attenuation is proportional to the standard deviation of the autocorrelation function, just as our calculated attenuation is proportional to κ_0^2 . However, they find that the attenuation is also proportional to the wavelength, which is not the case in our highly multimode ray-based picture. Another point that differentiates our work is our emphasis on refractive index-based optimization strategies to reduce the attenuation.

Funding. Grant number W911NF-19-1-0352 from the United States Army Research Office.

-
- [1] E. Witten, “Dynamical breaking of supersymmetry,” Nucl. Phys. B **188**, 513–554 (1981).
 - [2] E. Witten, “Supersymmetry and Morse theory,” J. Diff. Geom. **17**, 661–692 (1982).
 - [3] F. Cooper, A. Khare and U. Sukhatme, “Supersymmetry and Quantum Mechanics,” Phys. Rept. **251**, 267–385 (1995).
 - [4] F. Cooper and B. Freedman, “Aspects of supersymmetric quantum mechanics,” Ann. Phys. **146**, 262–288 (1983).
 - [5] F. Cooper, A. Khare, and U. Sukhatme, *Supersymmetry in quantum mechanics* (World Scientific, Singapore, 2001).
 - [6] S. M. Chumakov and K. B. Wolf, “Supersymmetry in Helmholtz optics,” Phys. Lett. A **193**, 51–53 (1994).
 - [7] G. Junker, *Supersymmetric methods in quantum and statistical physics*, (Springer-Verlag, Berlin, 2012).
 - [8] M. A. Jafarizadeh and H. Fakhri, “Supersymmetry and shape invariance in differential equations of mathematical physics,” Phys. Lett. A **230**, 164–170 (1997).
 - [9] R. Dutt, A. Khare, and U. P. Sukhatme, “Supersymmetry, shape invariance, and exactly solvable potentials,” Am. J. Phys. **56**, 163–168 (1988).
 - [10] R. Dutt, A. Khare, and U. P. Sukhatme, “Supersymmetry-inspired WKB approximation in quantum mechanics,” Am. J. Phys. **59**, 723–727 (1991).
 - [11] M. R. Zirnbauer, “The supersymmetry method of random matrix theory,” arXiv preprint math-ph/0404057 (2004).
 - [12] K. Efetov, *Supersymmetry in disorder and chaos*, (Cambridge University Press, New York, 1999).
 - [13] R. El-Ganainy, K. G. Makris, and D. N. Christodoulides, “Local PT invariance and supersymmetric parametric oscillators,” Phys. Rev. A **86**, 033813 (2012).
 - [14] M. A. Miri, M. Heinrich, R. El-Ganainy, and D. N. Christodoulides, “Supersymmetric optical structures,” Phys. Rev. Lett. **110**, 233902 (2013).
 - [15] M. A. Miri, M. Heinrich, and D. N. Christodoulides, “Supersymmetry-generated complex optical potentials with real spectra,” Phys. Rev. A **87**, 043819 (2013).
 - [16] M. Heinrich, M. A. Miri, S. Stützer, R. El-Ganainy, S. Nolte, A. Szameit, and D. N. Christodoulides, “Supersymmetric mode converters,” Nat. Commun. **5**, 3698 (2014).
 - [17] M. Heinrich, M. A. Miri, S. Stützer, S. Nolte, D. N. Christodoulides, and A. Szameit, “Observation of supersymmetric scattering in photonic lattices,” Opt. Lett. **39**, 6130–6133 (2014).
 - [18] M. A. Miri, M. Heinrich, and D. N. Christodoulides, “SUSY-inspired one-dimensional transformation optics,” Optica **1**, 89–95 (2014).
 - [19] R. El-Ganainy, L. Ge, M. Khajavikhan, and D. N. Christodoulides, “Supersymmetric laser arrays,” Phys. Rev. A **92**, 033818 (2015).
 - [20] W. Walasik, B. Midya, L. Feng, and N. M. Litchinitser, “Supersymmetry-guided method for mode selection and optimization in coupled systems,” Opt. Lett. **43**, 3758–3761 (2018).
 - [21] B. Midya, W. Walasik, N. M. Litchinitser, and L. Feng, “Supercharge optical arrays,” Opt. Lett. **43**, 4927–4930 (2018).
 - [22] B. Midya, H. Zhao, X. Qiao, P. Miao, W. Walasik, Z. Zhang, N. M. Litchinitser, and L. Feng, “Supersymmetric microring laser arrays,” Photon. Res. **7**, 363–367 (2019).
 - [23] W. Walasik, N. Chandra, B. Midya, L. Feng, and N. M. Litchinitser, “Mode-sorter design using continuous supersymmetric transformation,” Opt. Express **27**, 22429–22438 (2019).
 - [24] Q. Zhong, S. Nelson, M. Khajavikhan, D. N. Christodoulides, and R. El-Ganainy, “Bosonic dis-

- crete supersymmetry for quasi-two-dimensional optical arrays,” *Photon. Res.* **7**, 1240–1243 (2019)
- [25] M. P. Hokmabadi, N. S. Nye, R. El-Ganainy, D. N. Christodoulides, and M. Khajavikhan, “Supersymmetric laser arrays,” *Science* **363**(6427), 623–626 (2019).
- [26] G. Parisi, and N. Sourlas, “Random magnetic fields, supersymmetry, and negative dimensions,” *Phys. Rev. Lett.* **43**, 744 (1979).
- [27] G. Parisi, and N. Sourlas, “Supersymmetric field theories and stochastic differential equations,” *Nucl. Phys. B* **206**, 321–332 (1982).
- [28] W. B. Gardner, “Microbending loss in optical fibers,” *Bell Labs Tech. J.* **54**, 457–465 (1975).
- [29] X. Jin and F. P. Payne, “Numerical investigation of microbending loss in optical fibres,” *J. Lightwave Technol.* **34**, 1247–1253 (2016).
- [30] B. E. A. Saleh and M. C. Teich, *Fundamentals of photonics*, (John Wiley & sons, New Jersey, 2019).
- [31] M. Heiblum and J. Harris, “Analysis of curved optical waveguides by conformal transformation,” *IEEE J. Quantum Electron.* **11**, 75–83 (1975).
- [32] R. A. Herrera, C. T. Law, and A. Mafi, “Calculation of the acousto-optic coupling coefficients in optical fibers,” *Opt. Commun.* **305**, 217–220 (2013).
- [33] M. Rousseau and J. Arnaud, “Ray theory of microbending,” *Opt. Commun.* **25**, 333–336 (1978).
- [34] J. Arnaud and M. Rousseau, “Ray theory of randomly bent multimode optical fibers,” *Opt. Lett.* **3**, 63–65 (1978).
- [35] D. Gloge and E. A. J. Marcatili, “Multimode theory of graded-core fibers,” *Bell. Syst. Tech. J.* **52**, 1563–1578 (1973).
- [36] A. Mafi, “Pulse propagation in a short nonlinear graded-index multimode optical fiber,” *J. Lightw. Technol.* **30** 2803–2811 (2012).
- [37] C. V. Sukumar, “Supersymmetric quantum mechanics of one-dimensional systems,” *J. Phys. A* **18**, L57–L61 (1985).
- [38] G. P. Agrawal, *Fiber-Optic Communication Systems*, 4th ed. (Wiley, New York, 2010), Chap. 2.7.
- [39] F. Grillot, L. Vivien, S. Laval, D. Pascal, and E. Casan, “Size influence on the propagation loss induced by sidewall roughness in ultrasmall SOI waveguides,” *IEEE Photon. Technol. Lett.* **16**, 1661–1663 (2004).